Interleukin-13 Displaying Retargeted Oncolytic Measles Virus Strains Have Significant Activity Against Gliomas With Improved Specificity

Cory Allen[1], **Georgia Paraskevakou**[1], **Ianko Iankov**[1], **Caterina Giannini**[2], **Mark Schroeder**[3], **Jann Sarkaria**[3], **Mark Schroeder**[3], **Raj K Puri**[4], **Stephen J Russell**[1], and **Evanthia Galanis**[1,5]

[1]Molecular Medicine Department, Mayo Clinic College Of Medicine, Rochester, Minnesota, USA

[2]Division of Anatomic Pathology, Mayo Clinic College Of Medicine, Rochester, Minnesota, USA

[3]Radiation Oncology Research, Mayo Clinic College Of Medicine, Rochester, Minnesota, USA

[4]US Food and Drug Administration, Rockville, Maryland, USA

[5]Department of Oncology, Mayo Clinic College Of Medicine, Rochester, Minnesota, USA

Abstract

The majority of glioblastoma multiforme (GBM) tumors (80%) overexpress interleukin-13 receptor α2 (IL-13Rα2), but there is no expression of IL-13Rα2 in normal brain. Vaccine strains of measles virus have significant antitumor activity against gliomas. We tested the hypothesis that measles virus entry could be retargeted via the IL-13Rα2. MV-GFP-H_{AA}-IL-13 was generated from the Edmonston-NSe vaccine strain, by displaying human IL-13 at the C-terminus of the H protein, and introducing CD46 and signaling lymphocyte activation molecule (SLAM)-ablating mutations in H. The IL-13 retargeted virus showed significant cytopathic effect (CPE) against IL-13Rα2 overexpressing glioma lines, and lack of CPE/viral replication in normal human astrocytes and normal human fibroblasts not expressing IL-13Rα2. *In vivo* treatment of orthotopically implanted GBM12 xenografts demonstrated significant prolongation of survival in mice treated with the retargeted strain ($P < 0.0001$), and comparable activity between the IL-13R retargeted strain and MV-GFP ($P = 0.6377$). In contrast to MV-GFP-treated mice, administration of the retargeted strain in the central nervous system of measles replication-permissive Ifnar^{ko} CD46 Ge mice resulted in lack of neurotoxicity. Strains of measles virus retargeted against the glioma-specific IL-13Rα2 receptor have comparable therapeutic efficacy, and improved specificity as compared with the unmodified measles virus strain MV-GFP *in vitro* and *in vivo*.

Introduction

Glioblastoma multiforme (GBM) is the most frequent primary brain tumor in adults and accounts for most of the 18,500 primary brain tumor cases diagnosed each year in the United States.[1] Standard of care in GBM treatment includes a multimodality approach incorporating surgery, chemotherapy, and radiation therapy. Despite aggressive management, GBM invariably recur and prognosis remains dismal with a median survival of only 3–5 months at recurrence. Novel therapeutic approaches in this setting are urgently needed.

Correspondence: Evanthia Galanis, Division of Medical Oncology, Mayo Clinic College Of Medicine, 200 First Street, SW, Rochester, Minnesota 55905, USA. E-mail: galanis.evanthia@mayo.edu.

We have previously demonstrated that attenuated measles virus strains derived from the Edmonston vaccine lineage have antitumor activity against gliomas.[2] A strain of the virus expressing the human carcinoembryonic antigen (MV-CEA) is currently in phase I testing in patients with recurrent GBM.

Measles virus is a negative strand RNA virus that enters human cells through two known receptors: CD46, a regulator of complement activation that is ubiquitously expressed in human cells,[3,4] but overexpressed in tumors including GBM,[5] and signaling lymphocyte activation molecule (SLAM) (signaling lymphocyte-activated molecule) expressed on activated B and T cells and macrophages.[6–8]

Potential challenges in the clinical application of oncolytic measles virus strains as glioma therapeutics are the ubiquitous, although low level, expression of CD46 in normal brain and blood–brain barrier[9,10] and the interaction with SLAM, which has been associated with immunosuppression after infection with wild-type virus.[6,7] Retargeting of measles strains against glioma-specific receptors could therefore further improve viral specificity, and assist us in overcoming possible variability in CD46 expression in a therapeutic setting.[11]

Identification of measles H protein mutations that ablate entry via CD46 and SLAM[12,13] has allowed measles virus retargeting when combined with display of single-chain antibodies at the C-terminus of H.[14–16] Retargeting of the measles virus by cytokine display has not been accomplished, however.

Approximately 80% of GBM tumors express the IL-13 receptor, IL-13Rα2.[17–19] This receptor is not expressed in normal brain,[18,19] and it therefore represents an excellent glioma target. IL-13Rα2 is a monomer, binds to IL-13, and has a short cytoplasmic domain,[18–20] which at least in macrophages signals via AP-1.[21] However, the role of IL-13Rα2 expression in glioma cells and its mechanism of signaling remains unclear.

We hypothesized that engineering measles virus to enter via the IL-13Rα2 receptor by displaying human IL-13 and ablating natural viral entry via CD46 and SLAM could increase tumor specificity without decreasing antitumor efficacy. IL-13 display has been used to target DNA viruses such as conditionally replication-competent HSV-1 strains[22] or adenovirus.[23] Optimization is still needed, however, given the low titers of the retargeted herpes strains,[22] while the IL-13 displaying adenoviral vectors still maintained entry through the natural CAR. [23]

We constructed a human IL-13 displaying retargeted measles virus strain (MV-GFP-H$_{AA}$-IL-13) and demonstrated that it propagates in comparable titer to the unmodified strains and maintains equal potency both *in vitro* and *in vivo* against receptor expressing glioma cells. The retargeted virus demonstrated increased specificity as compared to the unmodified MV-GFP strain both in *in vitro* assays against nontransformed cells and in a central nervous system measles toxicity transgenic mouse model. This retargeted measles strain could therefore have significant applicability in glioma virotherapy.

Results

Construction and characterization of MV-GFP-H$_{AA}$-IL-13

We rescued the retargeted MV-GFP-H$_{AA}$-IL-13 virus, which derives from the Edmonston-NSe strain, and contains a single CD46 ablating mutation at position 481 and a single SLAM ablating mutation at position 533. The virus was rescued using the pseudoreceptor STAR system as described by Nakamura *et al.*[14] and propagated on Vero-His cells. The MV-GFP-H$_{AA}$-IL-13 virus displays IL-13 at the C-terminus of H protein coupled with a 6-histidine tag.

The latter modification enables rescue of retargeted virus using Vero-αHis cells. The virus also contains the green fluorescent protein (GFP) gene at position 1 which facilitates viral rescue and allows visualization of infection *in vitro* (Figure 1a). MV-GFP, expressing the unmodified H protein of the Edmonston-NSe strain and GFP at position 1 was used as the positive control. Western immunoblotting after infection of Vero-αHis (Figure 1b) confirmed the presence of the 84-kd chimeric H protein in the retargeted virus, and IL-13 expression (Figure 1c). Titers of the recombinant virus in the range of 3×10^7 50% tissue culture infective dose (TCID$_{50}$) were obtained, which is comparable with viral titers obtained for the unmodified MV-strains. One-step viral growth curves in permissive Vero-αHis cells demonstrated comparable kinetics between the retargeted and unmodified virus (Figure 1d).

In vitro infection of established and primary tumor cells with the retargeted strain is dependent on the expression level of IL-13Rα2 and results in comparable CPE to the unmodified strain MV-GFP in tumor cells expressing intermediate/high receptor levels

Expression of IL-13Rα2 was examined by flow cytometry and western immunoblotting in a panel of both primary and established cell lines. All glioma lines expressed in IL-13Rα2 receptor to varying degrees. In contrast, there was low or no expression of the IL-13Rα1 receptor (data not shown). In fluorescence-activated cell sorting data for IL-13Rα2 were quantified by calculating the mean FL1 peak shift when cells were incubated with the IL-13Rα2 antibody as compared to the isotype control (Figure 2a). Most of the primary and established glioma lines (10/14) had intermediate or high IL-13Rα2 expression. These data, which are consistent with IL-13Rα2 expression data in patient tumors emphasize the broad applicability of an IL-13 targeting strategy in the treatment of gliomas. The MV-GFP-H$_{AA}$-IL-13 virus had comparable infectivity to the unmodified MV-GFP virus in glioma lines expressing intermediate or high levels of the receptor but not in cells expressing low levels of the receptor (Figure 2a). Cell viability was quantified by trypan blue exclusion at multiple time points. Representative data for day 7 after infection are presented (Figure 2b). Cytotoxicity of MV-GFP-H$_{AA}$-IL-13 was comparable to MV-GFP in glioma lines expressing intermediate of high receptor levels (GBM12, U251, U87, GBM10, GBM39), but inferior to MV-GFP in glioma lines expressing low receptor levels (U118, GBM8).

The retargeted virus MV-GFP-H$_{AA}$-IL-13 depends on the interaction of the displayed IL-13 with the IL-13Rα2 receptor for the entry of virus and infection of tumor cells. To determine the specificity of MV-GFP-H$_{AA}$-IL-13 viral entry, U87 tumor cells, which express the IL-13Rα2, but not the IL-13Rα1 receptor were either left untreated or exposed to 1 or 30 ng/μl of IL-13, IL-2, or IL-4 for 1 hour before infection with the IL-13 retargeted or the unmodified virus. Pretreatment with 30 ng/μl IL-13 eliminated viral transduction as demonstrated by lack of GFP positivity (Figure 3a). In addition, there was a 3½ log decrease in MV-GFP-H$_{AA}$-IL-13 viral titers in cells pretreated with 30 ng/μl of IL-13 as compared with cells pretreated with IL-2, IL-4, or cytokine untreated cells. Pretreatment with either IL-2 or IL-4 did not affect MV-GFP-H$_{AA}$-IL-13 infectivity (Figure 3b). Furthermore, pretreatment with an IL-13Rα2-binding antibody decreased susceptibility to MV-GFP-H$_{AA}$-IL-13 infection (Figure 3c). These results collectively demonstrate the specificity of viral entry and replication in cells expressing IL-13Rα2.

IL-13 displaying measles virus strains has no CPE against nontransformed cells

Overexpression of IL-13Rα2 in GBM but not in normal tissues has been previously demonstrated.[17−19] Western immunoblotting was used to confirm the absence of IL-13Rα2 in both normal human astrocytes and normal human dermal fibroblasts (Figure 4a). In contrast to MV-GFP, exposure of both normal human astrocytes and normal human dermal fibroblasts to the MV-GFP-H$_{AA}$-IL-13 virus resulted in lack of infection as demonstrated by lack of GFP positivity (Figure 4b) and cytopathic effect (CPE) (Figure 4c) at multiple time points.

Furthermore, and in contrast to treatment with the unmodified strain MV-GFP, there was no expression of the measles virus nucleocapsid (N) protein in astrocytes or fibroblasts treated with the retargeted strain, similarly indicating lack of infection (Figure 4d).

IL-13Rα2 retargeted measles virus strains have comparable *in vivo* antitumor efficacy to the unmodified strain MV-GFP in an orthotopic tumor model expressing IL-13Rα2

To assess antitumor efficacy of the MV-GFP-H_{AA}-IL-13 virus *in vivo*, we used the GBM12 orthotopic tumor model in BalbC/nude mice. GBM12 is derived from a Mayo Clinic GBM patient, is propagated as subcutaneous xenografts in nude mice and maintains the histological and molecular characteristics of the human tumor it derives from [ref. 24]. GBM12 expresses high levels of the IL-13Rα2 receptor. GBM12 tumors were established after orthotopic implantation in BalbC/nude mice and treated intratumoraly with a total dose of 9×10^5 TCID$_{50}$ of either MV-GFP or MV-GFP-H_{AA}-IL-13 or ultraviolet (UV)-inactivated MV-GFP. Significant prolongation of survival was observed in both MV-GFP- and MV-GFP-H_{AA}-IL-13-treated mice. Of equal importance, the retargeted strain had comparable activity to the unmodified virus (UV-MV-GFP versus MV-GFP $P < 0.0001$; UV-MV-GFP versus MV-GFP-H_{AA}-IL-13 $P < 0.0001$; MV-GFP versus MV-GFP-H_{AA}-IL-13 $P = 0.6377$) (Figure 5a). Characteristic CPE with formation of syncytia was observed in hematoxylin and eosin sections of mouse brains treated with either MV-GFP or the retargeted strain MV-GFP-H_{AA}-IL-13 (Figure 5b).

MV-GFP-H_{AA}-IL-13 causes no neurotoxicity after intracerebral administration in MV-susceptible Ifnar[ko] CD46 Ge transgenic mice

Rodents do not express the measles virus receptors CD46 or SLAM. Our orthotopic efficacy model cannot therefore be used for assessment of viral toxicity. Ifnar[ko] CD46 Ge is a transgenic mouse strain susceptible to measles virus infection. Although glioma lines are not tumorigenic in Ifnar[ko] CD46 Ge mice and as a result this model cannot be used for assessment of efficacy, it represents an excellent model for comparative assessment of measles toxicity.[25–27] Intracerebral administration of MV Edmonston strain in these mice results in the development of lethal encephalitis.[25,26] Given the significant degree of homology between mouse and human IL-13Rα2 receptor[28,29] and the lack of species specificity of IL-13, Ifnar[ko] CD46 Ge mice represent a suitable model for assessment of MV-GFP-H_{AA}-IL-13-induced toxicity. Following a single orthotopic administration of 1×10^5 TCID$_{50}$ of either MV-GFP or MV-GFP-H_{AA}-IL-13 in Ifnar[ko] CD46 GE mice, four of five mice administered the unmodified MV-GFP virus had to be euthanized within a week due to development of significant neurotoxicity, while complete lack of neurotoxicity was observed in mice injected with the retargeted strain MV-GFP-H_{AA}-IL-13 (Figure 6a), thus indicating an improved therapeutic index. Brain tissue overlay on Vero-αHis cells resulted in abundant virus rescue from brains of MV-GFP-treated animals. No virus was recovered from animals treated with the MV-GFP-H_{AA}-IL-13 virus (Figure 6b). Histopathological examination demonstrated inflammation at the injection site, meningitis with syncytia formation, and ventriculitis in the brains of MV-GFP-treated animals, but normal brain histology in the MV-GFP-H_{AA}-IL-13 virus-treated mouse (Figure 6c).

Discussion

Current multimodality therapy employed the treatment of GBM has dismal outcome resulting in a median survival of only 12–16 months. Novel therapeutic approaches are necessary to improve the outcome of GBM patients. Exploiting tumor-specific targets to develop glioma-targeted therapeutics represents a direction worth exploiting further.[30]

We have previously demonstrated that measles virus vaccine strains have significant antitumor activity against gliomas[2] and we have recently initiated a phase I trial of intratumoral and resection cavity administration of a measles virus derivative expressing the human

carcinoembryonic antigen (MV-CEA) in patients with recurrent GBM. Retargeting against glioma-specific receptors could further improve safety and allow us to overcome potential issues associated with variable expression of measles virus receptor CD46 in high-grade gliomas.[5]

Measles virus entry is mediated by the two glycoproteins of the viral envelope: the hemagluttanin H that mediates attachment to one of the two known measles virus receptors CD46 ([ref. 3]) or SLAM,[8] and the F (fusion) protein. To retarget fusion effectively against glioma-specific targets, the new specificity domain displayed on H protein should preserve its ability to trigger conformational changes in the F protein, when combined with mutations blocking entry through the natural receptors CD46 and SLAM.[14,15] The only display platform so far that has allowed retargeting has been the display of single-chain antibodies at the C-terminus of H protein.[13−16] Our results serve as the first demonstration that true retargeting of the measles virus can also be accomplished by displaying cytokines, such as the human IL-13 at the C-terminus of H protein. The MV-GFP-H_{AA}-IL-13 virus enters cells by its interaction with the IL-13Rα2 receptor as was demonstrated by competetive assay experiments in which depletion of the receptor from the cell surface by exposing the cells to 30 ng/ml of soluble IL-13 eliminates GFP positivity after infection with the retargeted strains and decreases viral yields by 3½ logs. Because IL-13Rα2 is internalized after binding IL-13, the receptor subsequently becomes unavailable for viral entry.[31,32] In contrast, pretreatment with IL-2 or IL-4 did not affect viral infectivity.

The monomeric IL-13Rα2 receptor represents an excellent glioma target, because it is overexpressed in 80–100% of high-grade gliomas,[17−19] but not in normal brain.[18,19] Expression of the receptor in normal human tissue is limited to testes.[18] Although it binds to IL-13 with high affinity, it does not mediate signaling through the STAT6 pathway.[31]

Although the primary and established glioma lines we screened had variable IL-13Rα2 receptor expression by fluorescence-activated cell sorting or western blotting, approximately 70% (10/14 lines) expressed intermediate or high receptor levels, and in these lines comparable therapeutic efficacy between retargeted and unmodified strains was observed. This is consistent with previous observations indicating that a certain receptor threshold is necessary for measles infection to result in extensive cell fusion and CPE.[33,34]

In contrast to the unmodified virus, retargeted strains were unable to infect nontransformed cells which do not express the IL-13Rα2 receptor such as normal human astrocytes and fibroblasts. In addition, orthotopic administration of the virus in Ifnar[ko] CD46 Ge mice, a very sensitive model of measles neurotoxicity, demonstrated lack of clinical neurotoxicity after administration of the IL-13 displaying retargeted virus, no viral recovery after overlay on Vero-αHis cells, and no histopathological changes. The mouse IL-13Rα2 receptor has significant homology to the human receptor[28,29] and IL-13 is not species specific: the lack of toxicity in the Ifnar[ko] CD46 Ge mice therefore, in conjunction with the efficacy data generated in the GBM12 orthotopic efficacy model support that measles retargeting by IL-13 display has decreased potential for toxicity without losing potency as compared with unmodified strains. It is of note that, in addition to gliomas, IL-13Rα2 is expressed in other tumor types such as ovarian cancer,[35] prostate cancer,[36] renal cell carcinoma, Kaposi's sarcoma and head and neck cancer,[37−39] thus increasing the potential applicability of this retargeted virotherapy approach.

IL-13 display has been used to retarget DNA viruses such as replicating herpes virus strains[22] and replication-deficient adenovirus.[12] In order to retarget herpes virus, IL-13 display was combined with mutations that disable viral binding to heparin sulfate proteoglycan, nectin 1, and HveA receptors.[22] Yields of this retargeted herpes virus (R5141) were significantly lower, however, relatively to those of the wild-type parent virus, and no data on *in vivo* testing

of this virus in animal models have been reported. The IL-13 displaying adenoviral vectors were replication deficient and they still maintained entry via the native CAR.[23] Our results demonstrate that retargeting of a replicating RNA vector by IL-13 display is feasible. Of equal importance, we were able to overcome some of the limitations pertaining to IL-13Rα2 targeting of DNA vectors; the retargeted strain maintained viral titers, and *in vivo* antitumor activity that was comparable to the unmodified strain. This in conjunction with the 70–80% expression of IL-13Rα2 in high-grade gliomas[17,18] potentially opens new directions in targeted glioma virotherapy.

IL-13 mutants have been generated, which demonstrate higher affinity for the IL-13Rα2 receptor. For example, substitution of a glutamine acid residue at position 13 with a lysine residue[40] resulted in an IL-13 mutant (IL-13 E13K)–binding receptor expressing tumor cells with a 3–10 times higher affinity as compared with IL-13. Nevertheless, when IL13E13K was fused to a *pseudomonas* exotoxin, this did not translate into superior antitumor efficacy as compared with the unmodified IL-13 fusion protein.[41] In a different experimental system, an IL-13 mutant incorporating a substitution in position 13–IL13E13Y, which results in 20 times higher affinity for the IL-13Rα2 receptor and 5 times lower affinity for the IL-13Rα1/IL-4 receptor, was shown to specifically target GBM cells when displayed on cytoxic T lymphocytes.[42] Our laboratory is currently investigating the role of IL-13 mutants in measles retargeting.

Using single-chain antibody display on the H protein we have previously retargeted oncolytic measles virus strains against other glioma targets such as epidermal growth factor receptor vIII (EGFRvIII)[15] and EGFR.[16] The focal expression of targets such as EGFRvIII, the expression of EGFR in normal cells, as well as the much higher percentage of high-grade gliomas expressing IL-13Rα2 (80% versus 40–50% for EGFR and 20–30% for EGFRvIII) makes MV-GFP-H$_{AA}$-IL-13 our preferred retargeted strain for additional clinical glioma applications.

In summary, we demonstrated that measles virus strains retargeted by combination of IL-13 display and ablation of entry through the natural CD46 and SLAM receptors had comparable therapeutic efficacy *in vitro* and *in vivo* to the unmodified measles virus strain MV-GFP against tumor cells expressing intermediate or high levels of the IL-13Rα2 receptor (~70% of established and patient-derived cell lines in our series) and demonstrate improved specificity against nontransformed cells, and in a measles neurotoxicity transgenic mouse model. These strains therefore represent excellent candidates for clinical translation.

Materials and Methods

Cell culture

Vero (African green monkey kidney cells), U87, U118, and U251 glioma cell lines were purchased from American Type Culture Collection. All cell lines were grown at 37 °C in media recommended by American Type Culture Collection in a humidified atmosphere of 5% CO_2. Vero-αHis cells were kindly provided by Dr. T. Nakamura and grown in Dulbecco's modified Eagle's medium containing 10% fetal bovine serum, 1× penicillin/streptomycin. Primary glioblastoma lines (GBM5, GBM6, GBM8, GBM10, GBM12, GBM14, GBM15, GBM38, GBM39, GBM43, and GBM44) were generated as previously described[24] and maintained as subcutaneous xenografts. To establish short-term cultures, xenografts were excised and placed in culture dishes where the tissue was initially minced with a scalpel and then mechanically disrupted to create a cell suspension. Following short-term culture of the tumor cells (3–7 days) in Dulbecco's modified Eagle's medium with 2.5% fetal bovine serum, 1× penicillin/streptomycin cells were either used for orthotopic implantation or further maintained in culture in Dulbecco's modified Eagle's medium containing 10% fetal bovine serum, 1× penicillin/streptomycin for *in vitro* studies. Normal human astrocytes and normal human dermal

fibroblasts (Cambrex, Baltimore, MD) were grown in AGM (Cambrex, Baltimore, MD) and FGM (Cambrex, Baltimore, MD) media respectively, as recommended by the supplier.

Construction of MV-GFP-HAA-IL-13

IL-13 was PCR amplified from the pCR2.1-IL13 plasmid containing the human IL-13 complementary DNA (kindly provided by Dr. R. Puri) using the following primers: 5′-GGCCCAGCCGGCCATGTCCCCAGGCCCTGTGCCTCCCTCTACAGCCCTCAGGGA GCTCATTGA-3′ and 5′-TATGCGGCCGCGTTGAACTGTCCCTCGCGAAAAAGT-3′. The purified PCR product was cloned into pCR2.1 (Invitrogen, Carlsbad, CA) and the sequence of the resultant plasmid, pCR2.1-IL13, was verified by fluorescent sequence analysis. Using *Sfi*I–*Not*I digestion/ligation the *Sfi*I–*Not*I fragment from pCR2.1-IL13 was subcloned into pCG-H$_{AA}$-H6 (provided by Dr. T. Nakamura) to create the pCG-H$_{AA}$-IL-13-H6 plasmid. The *Pac*I–*Spe*I fragment from pCG-H$_{AA}$-IL-13-H6 encodes a modified measles H sequence, which incorporates both a CD46 and a SLAM ablating mutation (Y481A, R533A respectively) and displays IL-13 on its C-terminus as well as a 6-histidine tag to facilitate rescue. After *Pac*I–*Spe*I digestion of pCG-H$_{AA}$-IL-13-H6, the *Pac*I–*Spe*I fragment was gel purified and subcloned into the full-length plasmid p(+)MV-GFP-NSe, using *Pac*I–*Spe*I digestion/ligation. The resultant full-length plasmid, p(+)MV-GFP-H$_{AA}$-IL-13-H6, was used to rescue the virus as described by Nakamura *et al*.[14]

In brief, 293-3-46 helper cells were transfected with p(+)MV-GFP-H$_{AA}$-IL-13-H6, pCG-L and pCG-N plasmids, using the Profection Mammalian Transfection System Calcium Phosphate kit (Promega, Madison, WI). Twenty-four hours after transfection the cells were harvested and overlaid on Vero-αHis cells. The 6-histidine tag at the C-terminus of H protein allows rescue and propagation of the virus using Vero-αHis cells stably transfected with a pDisplace (Invitrogen, Carlsbad, CA) plasmid to express a membrane-bound single-chain antibody that recognizes the 6-histidine peptide. MV-GFP, which was used as the unmodified virus control, was rescued as previously described[43] and propagated using Vero cells. Viral stocks were prepared by infecting the appropriate Vero cell line with measles virus at a multiplicity of infection (MOI) of 0.02 and incubating at 32°C, 5% CO_2. Virus was harvested by three freeze–thaw cycles from cellular substrate, and resuspended in Opti-MEM (Life Technologies, Carlsbad, CA) after the third serial passage. Titers were determined by $TCID_{50}$ titration on Vero-αHis or Vero respectively, as previous described.[2]

Western immunoblotting for detection of viral H protein

Vero and Vero-αHis cells were infected with MV-GFP or MV-GFP-H$_{AA}$-IL-13 at an MOI of 0.1 $TCID_{50}$. Forty-eight hours after infection, crude lysates were scraped into Opti-MEM and subjected to a single freeze–thaw cycle. Cellular debris was removed through centrifugation and recovered virus was placed in lysis buffer [50 mmol/l sodium pyrophosphate, 50 mmol/l sodium fluoride, 50 mmol/l sodium chloride, 5 mmol/l EDTA, 5 mmol/l EGTA, 100 mmol/l sodium orthovanadate, 10 mmol/l HEPES pH 7.4, 0.1% Triton X-100 containing complete protease inhibitor cocktail tablets (Roche, Penzberg, Germany)] and separated by sodium dodecyl sulfate polyacrylamide gel electrophoresis. The gel was transferred to nitrocellulose (Bio-Rad, Hercules, CA) and blocked overnight at 4 °C in 1× Casein (Vector, Burlingame, CA) in Tween–Tris-buffered saline (Tween–TBS) (10 mmol/l Tris, pH 8.0, 150 mmol/l NaCl, 0.05% Tween-20). The blot was then incubated with rabbit antiH cytoplasmic tail antiserum (1:10,000) (kindly supplied by R. Cattaneo) in Tween–TBS containing 0.5% non-fat dry milk at room temperature for 60 minutes. Blots were washed for 60 minutes in Tween–TBS and incubated with goat antirabbit horseradish peroxidase (HRP) (1:2,000; Pierce, Rockford, IL) in Tween–TBS containing 0.5% nonfat dry milk at room temperature for 60 minutes. After extensive washing, the blot was visualized with SuperSignal West Femto Chemiluminescent Substrate (Pierce, Rockford, IL).

Western immunoblotting for detection of viral N protein

One million normal human astrocyte, normal human dermal fibroblast, or tumor cells were plated in 10-cm dishes. The next day cells were infected at an MOI of 1.0 with MV-GFP or MV-GFP-H_{AA}-IL-13. Forty-eight hours after infection, cells were rinsed with phosphate-buffered saline and lysed in 1 ml of lysis buffer. Samples were subsequently sonicated and 10 µg total protein was separated by sodium dodecyl sulfate polyacrylamide gel electrophoresis. The gels were transferred to nitrocellulose (Bio Rad, Hercules, CA) and blocked overnight at 4 °C in 1× casein (Vector, Burlingame, CA) in Tween–TBS. The blot was then incubated with rabbit anti-N (1:10,000) (kindly supplied by R. Cattaneo) in Tween–TBS containing 0.5% nonfat dry milk at room temperature for 60 minutes, washed for 60 minutes in Tween–TBS and incubated with goat anti-rabbit HRP (1:2,000; Pierce, Rockford, IL) in Tween–TBS containing 0.5% nonfat dry milk at room temperature for 60 minutes. After extensive washing, the blot was visualized with SuperSignal West Femto Chemiluminescent Substrate (Pierce, Rockford, IL). An actin control blot was incubated with mouse anti-β-actin (1:50,000) (Sigma, St Louis, MO) in Tween–TBS containing 0.5% nonfat dry milk at room temperature for 60 minutes, washed for 60 minutes in Tween–TBS and incubated with goat anti-mouse HRP (1:5,000; Pierce, Rockford, IL) in Tween–TBS containing 0.5% nonfat dry milk for 60 minutes. After extensive washing, the blot was developed with SuperSignal West Femto Chemiluminescent Substrate (Pierce, Rockford, IL).

Western immunoblotting for detection of IL-13

Approximately 10^7 $TCID_{50}$ of either MV-GFP or MV-GFP-H_{AA}-IL-13 were layered onto a 60/20% sucrose–TNE buffer (10 mmol/l Tris pH 7.8, 100 mmol/l NaCl, 1 mmol/l EDTA) gradient and centrifuged at 27,000 rpm in a Beckman Optima L-90K ultracentrifuge using a SW28 rotor for 90 minutes. The interphase from each viral preparation was removed, placed into 20% sucrose–TNE buffer and centrifuged to precipitate the virus containing fractions. The resulting pellet was resuspended in lysis buffer and separated by sodium dodecyl sulfate polyacrylamide gel electrophoresis. The gel was transferred to polyvinylidene fluoride (Bio-Rad, Hercules, CA) and blocked overnight at 4 °C in 1× casein (Vector, Burlingame, CA) in Tween–TBS. The blot was then incubated with 2 µg/ml mouse anti-IL-13 (Abcam, Cambridge, MA) in Tween–TBS containing 0.5% nonfat dry milk at 4 °C overnight. Blots were washed for 60 minutes in Tween–TBS and incubated with goat anti-mouse HRP (1:2,000; Pierce, Rockford, IL) in Tween–TBS containing 0.5% nonfat dry milk at room temperature for 60 minutes. After extensive washing, the blot was visualized with SuperSignal West Femto Chemiluminescent Substrate (Pierce, Rockford, IL).

Western immunoblotting for detection of the IL-13Rα2 receptor

Ten micrograms of sonicated whole-cell lysate from tumor cells, NHA, and NHDF were separated by sodium dodecyl sulfate-polyacrylamide gel electrophoresis. The gels were transferred to polyvinylidene fluoride (Bio-Rad, Hercules, CA) and blocked overnight at 4 °C in 1× casein (Vector, Burlingame, CA) in Tween–TBS. The blot was then incubated with 5 µg/ml goat anti-human IL-13Rα2 (R&D Systems, Minneapolis, MN) in Tween– TBS containing 0.5% nonfat dry milk at room temperature for 60 minutes, washed for 60 minutes in Tween–TBS and incubated with goat anti-rabbit-HRP (1:2,000; Pierce, Rockford, IL) in Tween–TBS containing 0.5% nonfat dry milk at room temperature for 60 minutes. After extensive washing, the blot was visualized with SuperSignal West Femto Chemiluminescent Substrate (Pierce, Rockford, IL). An actin control blot was incubated with mouse anti-β actin (1:50,000) (Sigma, St Louis, MO), incubated with goat anti-mouse-HRP (1:2,000) (Pierce, Rockford, IL) and visualized with SuperSignal West Femto Chemiluminescent Substrate (Pierce, Rockford, IL).

Determination of IL-13Rα2 and IL-13 Rα1 levels by fluorescence-activated cell sorting

IL-13 Rα1 and IL-13 Rα2 expression was assessed in 14 glioma lines, either established (U87, U251, U118) or derived from Mayo Clinic patients and propagated as subcutaneous xenografts in nude mice (GBM5, GBM6, GBM8, GBM10, GBM12, GBM14, GBM15, GBM38, GBM39, GBM43, and GBM44). One million tumor cells were harvested, washed, and then incubated with goat anti-human IL-13Rα2 (R&D Systems, Minneapolis, MN) or IL-13 Rα1 antibody (Abcam). Cells were washed and then incubated with mouse anti-goat IgG-FITC. Nonimmune IgG-FITC was used as a control (Pierce, Rockford, IL). Washed cells were fixed in PBS containing 0.5% paraformaldehyde and analyzed on a Becton-Dickinson FACScan Plus cytometer. Analysis was performed using CellQuest software (BD Biosciences, San Diego, CA).

Assessment of viral replication in Vero, Vero-αHis, and tumor cell lines

Cells were plated in six-well plates in duplicate at a density of 10^5 cells/well. Cells were infected as described above at an MOI of 0.1 $TCID_{50}$ with either MV-GFP or MV-GFP-H_{AA}-IL-13 and harvested on days 1, 2, 4, 5, 6, and 7 after infection. Viral particles were released with two cycles of freezing/thawing and the viral titer was determined by determining the $TCID_{50}$ on Vero and Vero-αHis cells.

Antibody blocking assays

Following 1-hour preincubation of U87 cells with an antibody binding to IL-13Rα2 (0–10 μg/ml), the cells were infected with MV-GFP or MV-GFP-H_{AA}-IL-13 at an MOI of 0.1 $TCID_{50}$ in six-well plates. Forty-eight hours after infection, the number of GFP-positive syncytia were counted and expressed as the average number of infectious centers per well.

Assessment of CPE *in vitro*

Cells were plated in six-well plates in duplicate at a density of 5×10^5 cells/well (glioma lines) or 2.5×10^5 cells/well (NHA, NHDF). Twenty-four hours after plating, cells were infected at an MOI of 1.0 with either MV-GFP or MV-GFP-H_{AA}-IL-13 in 1 ml of Opti-MEM for 2 hours at 37 °C. At the end of the incubation period, the virus was removed and the cells were maintained in their standard medium. The number of viable cells in each well was counted using a hemacytometer at 3, 5, 7, 9, and 11 days after infection using trypan blue exclusion. The percentage of surviving cells was calculated by dividing the number of viable cells in the infected well by the number of viable cells in uninfected wells corresponding to the same time point. Infection was confirmed using fluorescent microscopy at corresponding time points.

Assessment of viral entry specificity

U87 cells were plated in six-well plates in duplicate at a density of 10^5 cells/well. The next day cells were exposed to 1 or 30 ng/ml of IL-2, IL-4, or IL-13 (Chemicon, Temecula, CA) for 1 hour. Controls included both uninfected cells and infected cells without cytokine pretreatment. The cells were infected at an MOI of 0.1 $TCID_{50}$ with either MV-GFP or MV-GFP-H_{AA}-IL-13-H6 and harvested 3 days after infection. Viral particles were released with two cycles of freeze/thawing. The viral titer was determined by 50% tissue culture infective dose on Vero or Vero-αHis cells. Experiments were repeated twice.

Orthotopic in vivo experiments

All animal experiments were approved by the Mayo Institutional Animal Care and Use Committee. IL-13Rα2 expressing GBM12 orthotopic xenografts were developed by implantation of 3×10^5 GBM12 cells into the right caudate nucleus of 5-week-old BALB/c mice, using a small animal stereotactic frame (ASI Instruments, Warren, MI). Treatment was

initiated 4 days after implantation by intratumoral injection using the same coordinates as for implantation. Approximately 1×10^5 TCID$_{50}$/dose were administered in 10 μl three times per week over a 3-week period for a total dose of 9×10^5 TCID$_{50}$. The following groups were included (eight to nine animals each): UV-inactivated MV-GFP, MV-GFP, or MV-GFP-H$_{AA}$-IL-13. Mice were observed daily and were killed when neurological impairment or >10% weight loss was observed. The experiment was terminated at 45 days after implantation. Brains of killed animals were fixed in paraformaldehyde and embedded in paraffin for subsequent analysis.

Assessment of central nervous system toxicity in a measles replication-susceptible Ifnarko CD46 Ge transgenic mouse model

Measles virus strains cannot normally infect rodent cells because of lack of expression of measles virus receptors. We therefore used a measles infection-susceptible transgenic mouse model, the Ifnar[ko] CD46 Ge mice[25,26] to evaluate the neurotoxicity of the unmodified and retargeted measles strains. MV-GFP or MV-GFP-H$_{AA}$-IL-13 was orthotopically administered into the right caudate nucleus of 4–6 week-old Ifnar[ko] CD46 Ge transgenic mice using the small animal stereotactic frame (ASI Instruments, Warren, MI) with a 26-gauge Hamilton syringe, at a dose of 1×10^5 TCID$_{50}$. Five animals were included per group. The mice were followed for survival and were killed when neurological impairment was observed. Brains were removed, half paraffin embedded and half sliced, rinsed with PBS and overlaid on Vero and Vero-αHis cells for recovery of virus.

Statistical analysis

To assess animal survival, Kaplan–Meir curves were generated. The survival of mice in the different treatment groups was compared using the log-rank test. A *P* value of <0.05 was considered statistically significant.

Acknowledgments

References

1. Jemal A, Murray T, Ward E, Samuels A, Tiwari RC, Ghafoor A, et al. Cancer statistics, 2005. CA Cancer J Clin 2005;55:10–30. [PubMed: 15661684]

2. Phuong LK, Allen C, Peng KW, Giannini C, Greiner S, TenEyck CJ, et al. Use of a vaccine strain of measles virus genetically engineered to produce carcinoembryonic antigen as a novel therapeutic agent against glioblastoma multiforme. Cancer Res 2003;63:2462–2469. [PubMed: 12750267]

3. Dorig RE, Marcil A, Chopra A, Richardson CD. The human CD46 molecule is a receptor for measles virus (Edmonston strain). Cell 1993;75:295–305. [PubMed: 8402913]

4. Naniche D, Varior-Krishnan G, Cervoni F, Wild TF, Rossi B, Rabourdin-Combe C, et al. Human membrane cofactor protein (CD46) acts as a cellular receptor for measles virus. J Virol 1993;67:6025–6032. [PubMed: 8371352]

5. Ulasov IV, Tyler MA, Zheng S, Han Y, Lesniak MS. CD46 represents a target for adenoviral gene therapy of malignant glioma. Hum Gene Ther 2006;17:556–564. [PubMed: 16716112]

6. Hahm B, Arbour N, Naniche D, Homann D, Manchester M, Oldstone MB. Measles virus infects and suppresses proliferation of T lymphocytes from transgenic mice bearing human signaling lymphocytic activation molecule. J Virol 2003;77:3505–3515. [PubMed: 12610126]

7. Schneider-Schaulies S, ter Meulen V. Modulation of immune functions by measles virus. Springer Semin Immunopathol 2002;24:127–148. [PubMed: 12503061]

8. Tatsuo H, Ono N, Tanaka K, Yanagi Y. SLAM (CDw150) is a cellular receptor for measles virus. Nature 2000;406:893–897. [PubMed: 10972291]

9. McQuaid S, Cosby SL. An immunohistochemical study of the distribution of the measles virus receptors, CD46 and SLAM, in normal human tissues and subacute sclerosing panencephalitis. Lab Invest 2002;82:403–409. [PubMed: 11950898]

10. Shusta EV, Zhu C, Boado RJ, Pardridge WM. Subtractive expression cloning reveals high expression of CD46 at the blood-brain barrier. J Neuropathol Exp Neurol 2002;61:597–604. [PubMed: 12125738]

11. Maenpaa A, Junnikkala S, Hakulinen J, Timonen T, Meri S. Expression of complement membrane regulators membrane cofactor protein (CD46), decay accelerating factor (CD55), and protectin (CD59) in human malignant gliomas. Am J Pathol 1996;148:1139–1152. [PubMed: 8644856]

12. Vongpunsawad S, Oezgun N, Braun W, Cattaneo R. Selectively receptor-blind measles viruses: identification of residues necessary for SLAM- or CD46-induced fusion and their localization on a new hemagglutinin structural model. J Virol 2004;78:302–313. [PubMed: 14671112]

13. Nakamura T, Peng KW, Vongpunsawad S, Harvey M, Mizuguchi H, Hayakawa T, et al. Antibody-targeted cell fusion. Nat Biotechnol 2004;22:331–336. [PubMed: 14990955]

14. Nakamura T, Peng KW, Harvey M, Greiner S, Lorimer IA, James CD, et al. Rescue and propagation of fully retargeted oncolytic measles viruses. Nat Biotechnol 2005;23:209–214. [PubMed: 15685166]

15. Allen C, Vongpunsawad S, Nakamura T, James CD, Schroeder M, Cattaneo R, et al. Retargeted oncolytic measles strains entering via the EGFRvIII receptor maintain significant antitumor activity against gliomas with increased tumor specificity. Cancer Res 2006;66:11840–11850. [PubMed: 17178881]

16. Paraskevakou G, Allen C, Nakamura T, Zollman P, James CD, Peng KW, et al. Epidermal growth factor receptor (EGFR)-retargeted measles virus strains effectively target EGFR- or EGFRvIII expressing gliomas. Mol Ther 2007;15:677–686. [PubMed: 17299404]

17. Caput D, Laurent P, Kaghad M, Lelias JM, Lefort S, Vita N, et al. Cloning and characterization of a specific interleukin (IL)-13 binding protein structurally related to the IL-5 receptor alpha chain. J Biol Chem 1996;271:16921–16926. [PubMed: 8663118]

18. Debinski W, Gibo DM. Molecular expression analysis of restrictive receptor for interleukin 13, a brain tumor-associated cancer/testis antigen. Mol Med 2000;6:440–449. [PubMed: 10952023]

19. Debinski W, Gibo DM, Hulet SW, Connor JR, Gillespie GY. Receptor for interleukin 13 is a marker and therapeutic target for human high-grade gliomas. Clin Cancer Res 1999;5:985–990. [PubMed: 10353730]

20. Mintz A, Gibo DM, Slagle-Webb B, Christensen ND, Debinski W. IL-13Ralpha2 is a glioma-restricted receptor for interleukin-13. Neoplasia 2002;4:388–399. [PubMed: 12192597]

21. Fichtner-Feigl S, Strober W, Kawakami K, Puri RK, Kitani A. IL-13 signaling through the IL-13alpha2 receptor is involved in induction of TGF-beta1 production and fibrosis. Nat Med 2006;12:99–106. [PubMed: 16327802]

22. Zhou G, Roizman B. Construction and properties of a herpes simplex virus 1 designed to enter cells solely via the IL-13alpha2 receptor. Proc Natl Acad Sci USA 2006;103:5508–5513. [PubMed: 16554374]

23. Ulasov IV, Tyler MA, Han Y, Glasgow JN, Lesniak MS. Novel recombinant adenoviral vector that targets the interleukin-13 receptor alpha2 chain permits effective gene transfer to malignant glioma. Hum Gene Ther 2007;18:118–129. [PubMed: 17328684]

24. Giannini C, Sarkaria JN, Saito A, Uhm JH, Galanis E, Carlson BL, et al. Patient tumor EGFR and PDGFRA gene amplifications retained in an invasive intracranial xenograft model of glioblastoma multiforme. Neuro oncol 2005;7:164–176. [PubMed: 15831234]

25. Mrkic B, Odermatt B, Klein MA, Billeter MA, Pavlovic J, Cattaneo R. Lymphatic dissemination and comparative pathology of recombinant measles viruses in genetically modified mice. J Virol 2000;74:1364–1372. [PubMed: 10627547]

26. Mrkic B, Pavlovic J, Rulicke T, Volpe P, Buchholz CJ, Hourcade D, et al. Measles virus spread and pathogenesis in genetically modified mice. J Virol 1998;72:7420–7427. [PubMed: 9696838]

27. Roscic-Mrkic B, Schwendener RA, Odermatt B, Zuniga A, Pavlovic J, Billeter MA, et al. Roles of macrophages in measles virus infection of genetically modified mice. J Virol 2001;75:3343–3351. [PubMed: 11238860]

28. Hershey GK. IL-13 receptors and signaling pathways: an evolving web. J Allergy Clin Immunol 2003;111:677–690. [PubMed: 12704343]quiz 691

29. Wu AH, Low WC. Molecular cloning of the rat IL-13 alpha 2 receptor cDNA and its expression in rat tissues. J Neurooncol 2002;59:99–105. [PubMed: 12241113]

30. Simpson L, Galanis E. Recurrent glioblastoma multiforme: advances in treatment and promising drug candidates. Expert Rev Anticancer Ther 2006;6:1593–1607. [PubMed: 17134364]

31. Kawakami K, Taguchi J, Murata T, Puri RK. The interleukin-13 receptor alpha2 chain: an essential component for binding and internalization but not for interleukin-13-induced signal transduction through the STAT6 pathway. Blood 2001;97:2673–2679. [PubMed: 11313257]

32. Feng N, Lugli SM, Schnyder B, Gauchag JF, Graber P, Schlagenhauf E, et al. The interleukin-4/interleukin-13 receptor of human synovial fibroblasts: overexpression of the nonsignaling interleukin-13 receptor alpha2. Lab Invest 1998;78:591–602. [PubMed: 9605184]

33. Anderson BD, Nakamura T, Russell SJ, Peng KW. High CD46 receptor density determines preferential killing of tumor cells by oncolytic measles virus. Cancer Res 2004;64:4919–4926. [PubMed: 15256464]

34. Hasegawa K, Nakamura T, Marks JD, Russell SJ, Peng KW. Effect of ligand binding affinity and receptor density in relation to biology of retargeted viruses. Mol Ther 2006;13:S369.abstract 957

35. Kioi M, Kawakami M, Shimamura T, Husain SR, Puri RK. Interleukin-13 receptor a2 chain: a potential biomarker and molecular target for ovarian cancer therapy. Cancer 2006;107:1407–1418. [PubMed: 16902988]

36. Gonzalez-Moreno O, Calvo A, Joshi BH, Abasolo I, Leland P, Wang Z, et al. Gene expression profiling identifies IL-13 receptor alpha 2 chain as a therapeutic target in prostate tumor cells overexpressing adrenomedullin. Int J Cancer 2005;114:870–878. [PubMed: 15609296]

37. Husain SR, Puri RK. Interleukin-13 receptor-directed cytotoxin for malignant glioma therapy: from bench to bedside. J Neurooncol 2003;65:37–48. [PubMed: 14649884]

38. Obiri NI, Debinski W, Leonard WJ, Puri RK. Receptor for interleukin 13. Interaction with interleukin 4 by a mechanism that does not involve the common gamma chain shared by receptors for interleukins 2, 4, 7, 9, and 15. J Biol Chem 1995;270:8797–8804. [PubMed: 7721786]

39. Joshi BH, Kawakami K, Leland P, Puri RK. Heterogeneity in interleukin-13 receptor expression and subunit structure in squamous cell carcinoma of head and neck: differential sensitivity to chimeric fusion proteins comprised of interleukin-13 and a mutated form of Pseudomonas exotoxin. Clin Cancer Res 2002;8:1948–1956. [PubMed: 12060640]

40. Debinski W, Gibo DM, Obiri NI, Kealiher A, Puri RK. Novel anti-brain tumor cytotoxins specific for cancer cells. Nat Biotechnol 1998;16:449–453. [PubMed: 9592393]

41. Kioi M, Kawakami K, Puri RK. Analysis of antitumor activity of an interleukin-13 (IL-13) receptor-targeted cytotoxin composed of IL-13 antagonist and Pseudomonas exotoxin. Clin Cancer Res 2004;10:6231–6238. [PubMed: 15448012]

42. Kahlon KS, Brown C, Cooper LJ, Raubitschek A, Forman SJ, Jensen MC. Specific recognition and killing of glioblastoma multiforme by interleukin 13-zetakine redirected cytolytic T cells. Cancer Res 2004;64:9160–9166. [PubMed: 15604287]

43. Duprex WP, McQuaid S, Hangartner L, Billeter MA, Rima BK. Observation of measles virus cell-to-cell spread in astrocytoma cells by using a green fluorescent protein-expressing recombinant virus. J Virol 1999;73:9568–9575. [PubMed: 10516065]
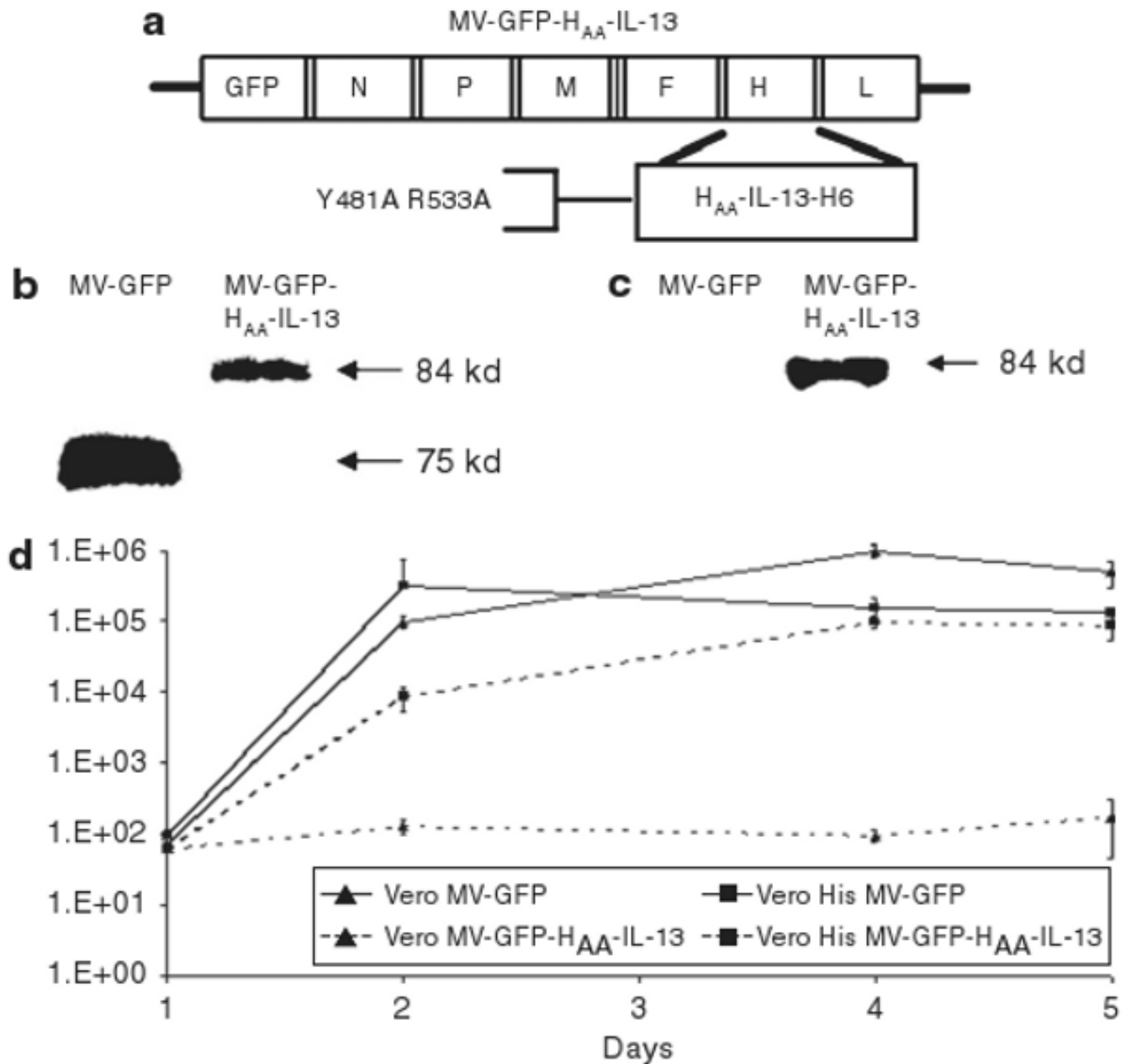
Figure 1. Construction of MV-GFP-H$_{AA}$-IL-13

(**a**) Schematic representation of the interleukin-13 (IL-13) receptor α2-retargeted virus. The hemagglutinin (H) protein contains both CD46 and signaling lymphocyte activation molecule–ablating mutations (Y481A and R533A, respectively). IL-13 is displayed on the C-terminus of H protein. The virus also contains the gene encoding green fluorescent protein (GFP) in position 1. (**b**) Expression levels of viral H protein were determined by western immunoblotting. The retargeted virus expresses chimeric H protein with higher molecular weight (84 kd as compared with 75 kd for the unmodified H protein). Expression levels of IL-13 in viral preparations were determined by western immunoblotting. In contrast to the unmodified virus MV-GFP, the MV-GFP-H$_{AA}$-IL-13 virus expresses IL-13. (**d**) Comparable

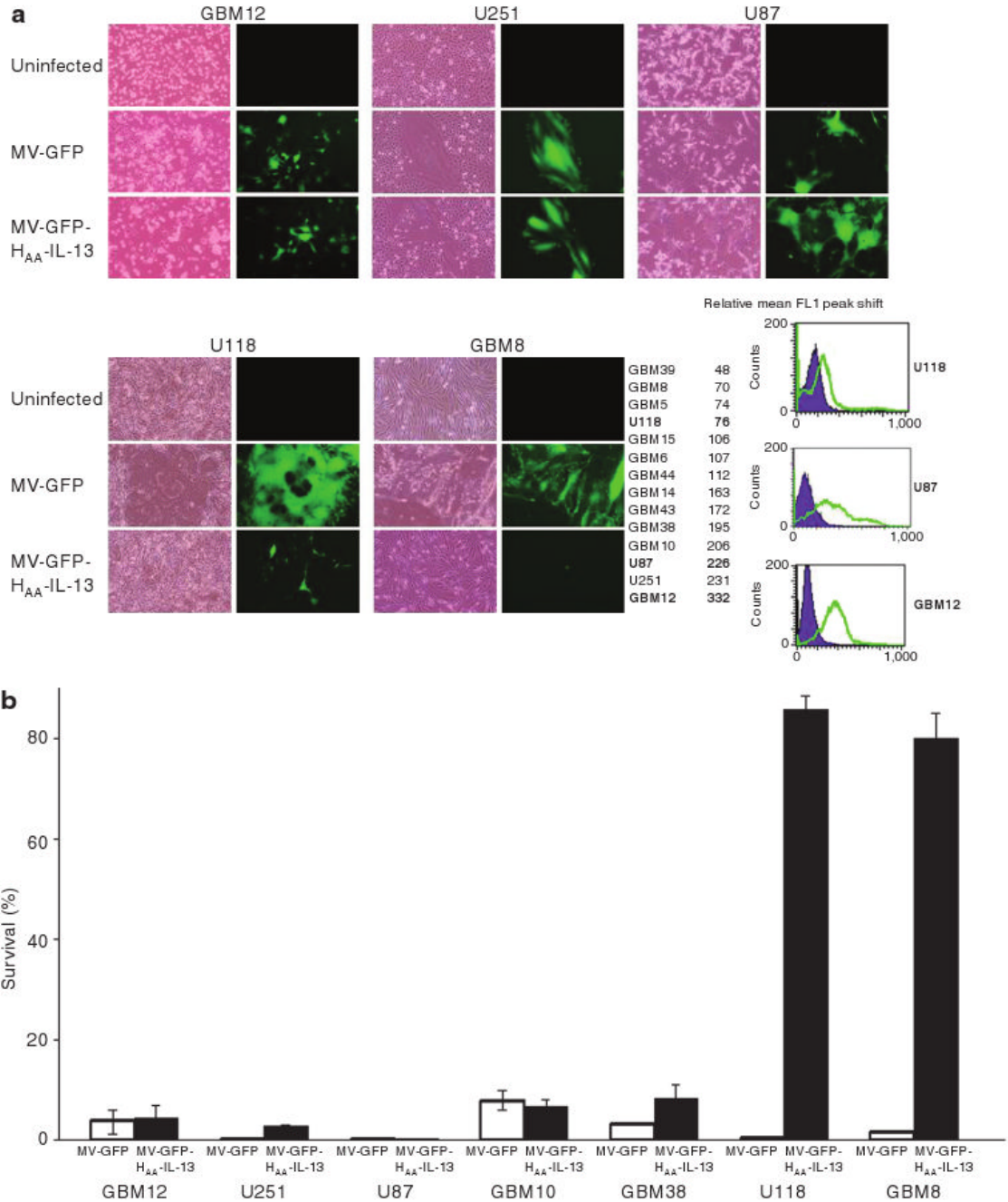replication of the MV-GFP H$_{AA}$-IL-13 virus to the unmodified MV-GFP virus was demonstrated in Vero-αHis cells.

Figure 2. MV-GFP-H$_{AA}$-IL-13 infectivity *in vitro*
(**a**) The MV-GFP-H$_{AA}$-IL-13 retargeted strain has comparable infectivity to the unmodified MV-GFP virus in glioma lines expressing intermediate or high levels of the interleukin-13 (IL-13) receptor α2 (IL-13Rα2) (GBM12, U251, U87), but not in glioma lines expressing low receptor levels (U118, GBM8) as demonstrated by expression of the green fluorescent protein and syncytia formation after viral infection (multiplicity of infection 1). (**b**) Cytopathic effect in glioma lines after infection with MV-GFP-H$_{AA}$-IL-13 and MV-GFP was quantitated by trypan blue exclusion assays at multiple time points. There was comparable cytotoxicity between the IL-13 displaying and the unmodified virus in tumor cell lines expressing

intermediate or high level of the IL-13Rα2 receptor (GBM12, U251, U87, GBM10, GBM38). Representative data on day 7 are shown. GBM, glioblastoma multiforme.
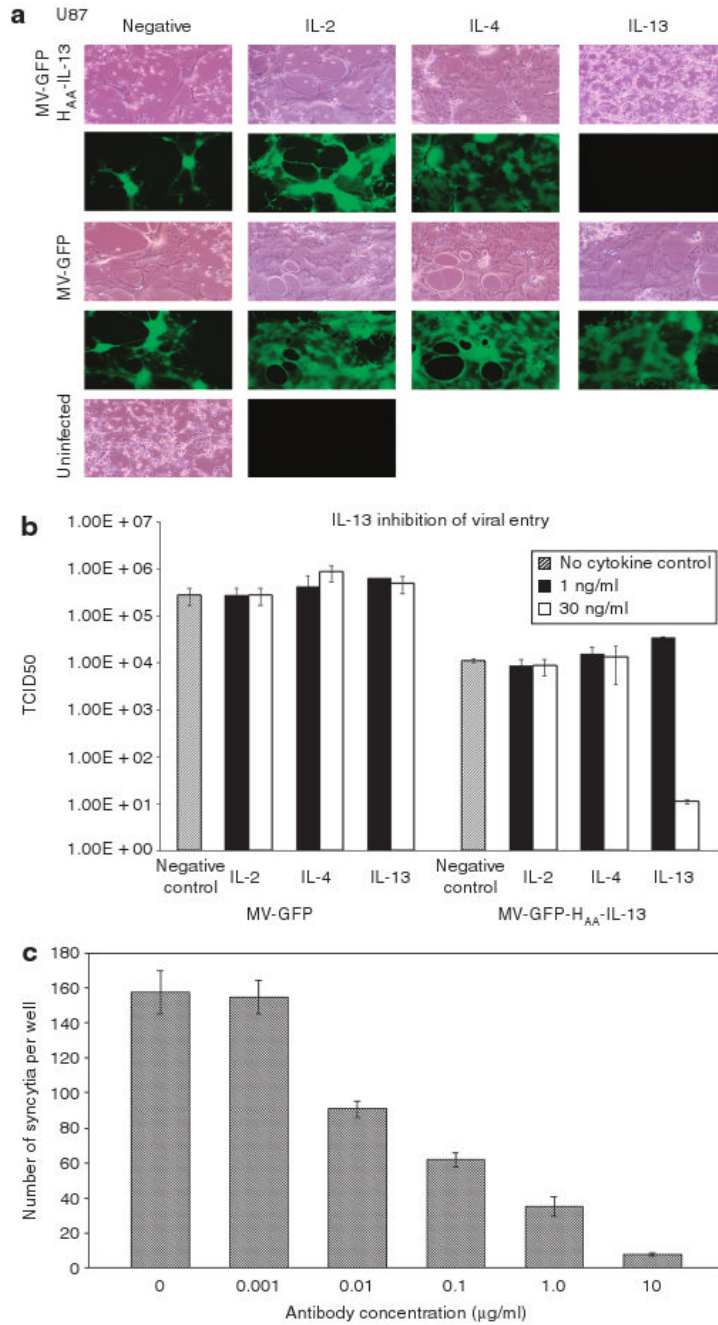
Figure 3. MV-GFP-H$_{AA}$-IL-13 entry is interleukin-13 receptor α2 (IL-13Rα2) dependent
Pre-exposure of IL-13Rα2 expressing U87 cells to IL-13 (30 ng/ml) precludes infection (**a**) and decreases replication of the MV-GFP-H$_{AA}$-IL-13 virus by 3½ logs (**b**). In contrast, pre-exposure of U87 cells to lower concentrations of IL-13 (1 ng/ml) or different cytokines such as IL-2 or IL-4 had no affect on viral infection or replication, indicating specificity of viral entry in IL-13Rα2-expressing tumor cells. Similarly, preincubation with an IL-13Ra2 antibody blocks infection with MV-GFP-H$_{AA}$-IL-13 (**c**). GFP, green fluorescent protein.
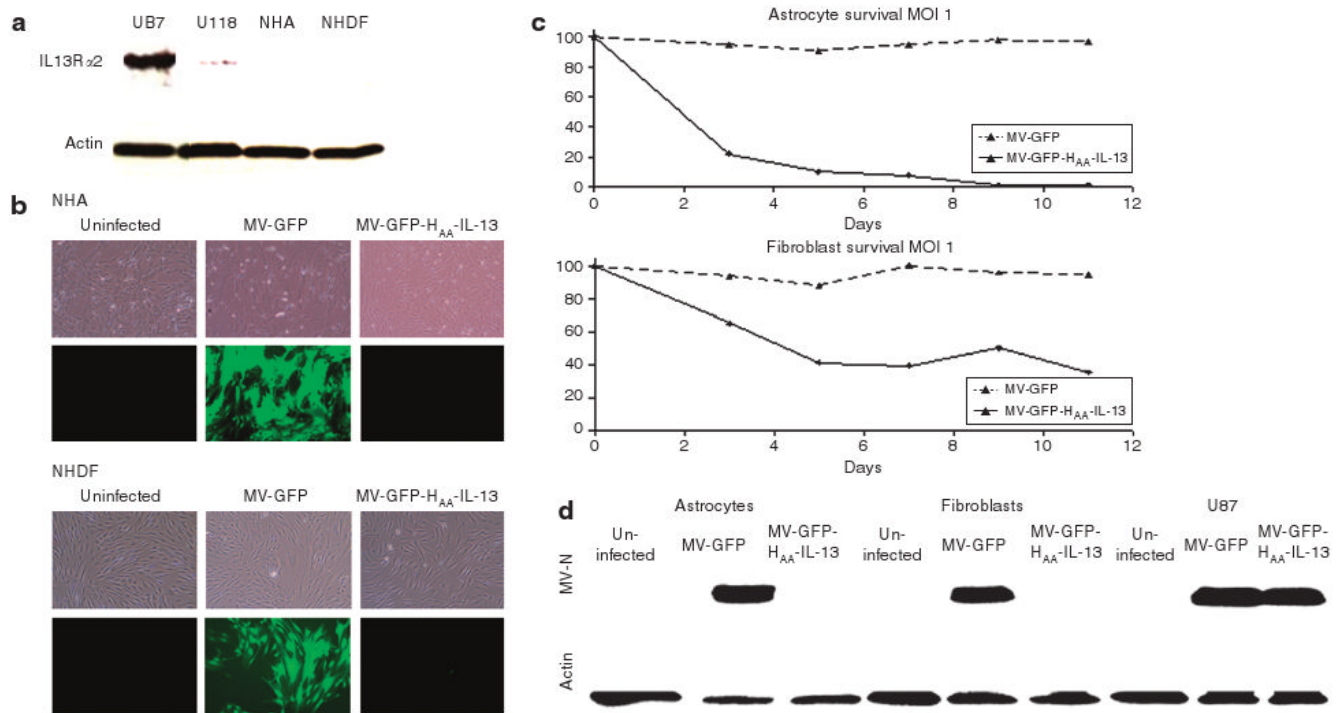
Figure 4. Lack of MV-GFP-H$_{AA}$-IL-13 cytopathic effect in normal (nontumor) cells
(**a**) Western immunoblotting of lysates derived from normal human astrocytes and fibroblasts shows lack of expression of the interleukin-13 (IL-13) receptor α2 (IL-13Rα2). U87 cells expressing high levels of IL-13Rα2 and U118 cells (low expressors) were used as controls. (**b**) In contrast to infection with MV-GFP, treatment of normal human astrocytes and fibroblasts with MV-GFP-H$_{AA}$-IL-13 virus did not cause infection or fusion [multiplicity of infection (MOI) 1.0, 72 hours after infection). (**c**) Cell viability of normal human astrocytes and fibroblasts in response to infection with MV-GFP-H$_{AA}$-IL-13 and MV-GFP was determined by trypan blue exclusion assays and presented as percentage of uninfected cells. In contrast to MV-GFP, the IL-13 displaying retargeted strain had no significant cytopathic effect (MOI 1.0). (**d**) Western immunoblotting for the measles virus nucleocapsid N protein was performed in cell lysates derived from primary glioblastoma multiforme lines, normal human astrocytes, and fibroblasts 48 hours after viral infection with either MV-GFP or MV-GFP-H$_{AA}$-IL-13 (MOI 1.0). In contrast to MV-GFP infection, there was no expression of measles virus N protein after treatment of normal human astrocytes and fibroblasts with the IL-13 displaying retargeted strain, thus indicating lack of infection. In contrast, in the IL-13Rα2-positive line U87 there is abundant N protein expression after infection with the retargeted strain. GFP, green fluorescent protein.
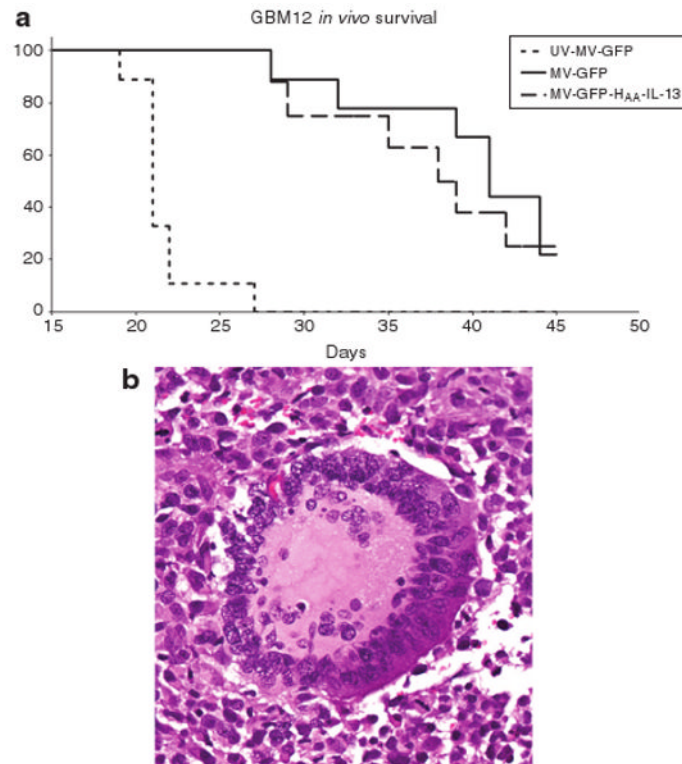
Figure 5. MV-GFP-H$_{AA}$-IL-13 has significant antitumor activity *in vivo*
(**a**) Antitumor effect of measles virus strain displaying interleukin-13 (IL-13) in the orthotopic animal model glioblastoma multiforme 12 (GBM12) that overexpresses interleukin-13 (IL-13) receptor α2. The MV-GFP-H$_{AA}$-IL-13 retargeted strain had significant antitumor activity which is comparable to the unmodified strain MV-GFP, resulting in significant propagation of survival in MV-GFP-H$_{AA}$-IL-13-treated animals ($P < 0.0001$) as compared with ultraviolet (UV)-inactivated virus. (**b**) Treatment induced cytopathic effect with syncytia formation observed in GBM12 xenografts treated with the MV-GFP-H$_{AA}$-IL-13 virus.
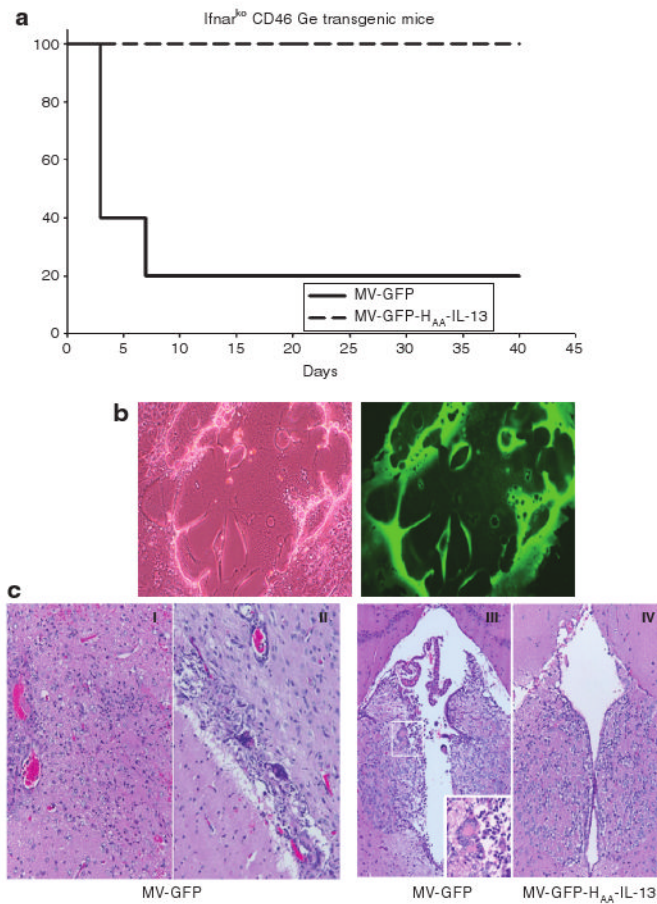
Figure 6. Lack of MV-GFP-H$_{AA}$-IL-13 toxicity in a susceptible transgenic mouse model
(**a**) Survival of Ifnar[ko] CD46 mice after central nervous system administration of MV-GFP or MV-GFP-H$_{AA}$-IL-13. In contrast to the lethal neurotoxicity observed by day 7 in four of five MV-GFP-treated mice, mice treated with the interleukin-13 (IL-13) displaying retargeted measles virus strain survived without toxicity. (**b**) Viral recovery from brains of MV-GFP-treated mice on Vero-αHis cell overlays as demonstrated by syncytia formation (I), expressing green fluorescence protein II. (**c**) Histopathological examination of the brains of MV-GFP-treated Ifnar[ko] CD46 Ge mice demonstrated inflammation at the injection site (I), meningitis (II), and ventriculitis (III) with syncytia formation (close-up view). In contrast, the brains of MV-GFP-H$_{AA}$-IL-13 mice have normal appearance on histopathological examination (IV).